 CMES, vol.3, no.6, pp.687-698, 2002

An Explicit Discontinuous Time Integration Method For Dynamic-Contact/Impact Problems

Jin Yeon Cho[1] **and Seung Jo Kim**[2]

Abstract: In this work, an explicit solution procedure for the recently developed discontinuous time integration method is proposed in order to reduce the computational cost while maintaining the desirable numerical characteristics of the discontinuous time integration method. In the present explicit solution procedure, a two-stage correction algorithm is devised to obtain the solution at the next time step without any matrix factorization. To observe the numerical characteristics of the proposed explicit solution procedure, stability and convergence analyses are performed. From the stability analysis, it is observed that the proposed algorithm gives a larger critical time step than the central difference method. From the convergence analysis, it is found that the present method with linear approximation in time gives the third order convergence that is higher than that of the central difference method. To check the performance of the proposed method in simulating impact problems, several numerical tests are carried out, and some of the results are compared with those obtained from the central difference method. Numerical tests show that the proposed explicit algorithm gives a much more robust numerical solution compared to the central difference method.

keyword: Dynamic-contact, Impact, Explicit Time Integration, Discontinuous Time Integration.

1 Introduction

Dynamic-contact/impact phenomena induce stiffness degradation and local failure of structural systems that lead directly to safety-related problems or malfunctions of high precision structures [Abrate (1991)]. For example, the impact on composite structures, used in aerospace applications, by a dropped tool or debris may cause invisible internal damage and a substantial drop in structural strength [Goo and Kim (1997)]. Therefore, the time dependent behavior of structures due to the impact of foreign objects should be predicted accurately. To analyze the transient dynamic behavior of structures, various numerical time integration methods have been suggested over the past several decades. However, it has been also reported in many studies that undesirable oscillations are produced in dynamic solutions when the previously developed time integration method is directly applied to the analysis of dynamic-contact/impact problems with impenetrability conditions alone. To alleviate the trouble, several works were carried out. Hughes, Taylor, Sackman, Curnier, and Kanoknukulchai (1976) employed the Newmark time integration method, and proposed the discrete dynamic-contact/impact conditions for a lumped-mass case to enforce the compatibility conditions of velocity and acceleration. Taylor and Papadopoulos (1993) assumed that the velocities and the accelerations on the contact points are independent of the displacements in the Newmark time integration method, and enforced the velocity and the acceleration compatibility. Lee (1994) proposed an iterative scheme to satisfy the velocity and acceleration compatibility on the contact surface for the constant average acceleration method, which is a special case of the Newmark time integration method.

Recently, for the analysis of the dynamic-contact/ impact problems, the discontinuous time integration method was proposed by Cho and Kim (1999). In respect to the fact that discontinuous function is utilized to approximate the dynamic filed variables, the discontinuous time integration method is similar to the time discontinuous Galerkin method [Hulbert and Hughes (1990); Chien and Wu (2001)] or time discontinuous approximation of weak Hamilton principle [Borri, Mello and Atluri (1990); Borri and Bottaso (1993)], while the starting point of the discontinuous time integration method is not a weak statement of dynamic equilibrium but an approximation of the relation between a function and its derivative like in conventional direct time integration. The dis-

[1] Department of Aerospace Engineering, INHA University, Korea
[2] Department of Aerospace Engineering, Seoul National University, Korea

continuous time integration method shows several desirable characteristics for simulations of impact problems. Since the algorithm allows jump discontinuity in field variables, it is suitable to depict abrupt changes of dynamic field variables according to shock loading produced in impact problems. The discontinuous time integration method does not produce undesirable oscillation, although undesirable oscillation is invoked when the constant average acceleration method or the central difference method is used as a time integration algorithm [Hughes, Taylor, Sackman, Curnier, Kanoknukulchai (1976); Taylor and Papadopoulos (1993); Zhong (1993); Lee (1994)]. Moreover it has a third order accuracy, while both the trapezoidal rule and the central difference method have only a second order accuracy [Hughes (1987)]. However, since the discontinuous time integration method is an implicit algorithm, its computational cost is more expensive than that of an explicit time integration method, such as the central difference method.

Thus, in this paper, an explicit solution procedure of the discontinuous time integration method is proposed in order to reduce the computational cost as well as preserve the desirable numerical features of the discontinuous time integration method. To avoid matrix factorization in this explicit solution algorithm, two-stage correction procedure is designed through the modification of the discontinuous time integration method. To observe the algorithmic features of the proposed explicit solution procedure, accuracy and stability analyses are carried out and several numerical simulations of impact problems are performed along with the exterior penalty method.

2 Discontinuous Time Integration Method

In this section, the recently proposed discontinuous time integration method [Cho and Kim (1999)] is briefly reviewed. In dynamic-contact/impact phenomena, the dynamic field variables are suddenly changed due to shock type loading. Therefore it is natural and reasonable to incorporate discontinuity in the time integration method. In the discontinuous time integration method, the concept of generalized derivative in distribution theory [Reddy (1986)] and jump assumption are considered together in order to depict the sudden change of dynamic field variables caused by the impact. The definition of a generalized derivative can provide the meaning of a derivative even for a discontinuous distribution like Dirac delta. The definition of a generalized derivative of distribution [Reddy (1986)] is constructed through integration-by-parts. By this procedure, the difficulty of differentiation of a distribution is transferred to the differentiation of a test function. Using the concept with jump assumption at the initial time, the generalized relation between the displacement vector $\mathbf{u}(t)$ and velocity vector $\mathbf{v}(t)$ is constructed by integration-by-parts, as shown below.

$$\int_{t_0}^{t_f} \mathbf{w}^T \mathbf{v} dt = -\int_{t_0}^{t_f} \dot{\mathbf{w}}^T \mathbf{u} dt + \mathbf{w}^T \mathbf{u}\Big|_{t_0}^{t_f} \quad \text{for all } \mathbf{w}(t) \tag{1}$$

where $\mathbf{w}$ denotes the test function. To describe the sudden changes of dynamic field variables naturally, the jump conditions at the initial time t_0 are assumed:

$$\mathbf{u}(t_0) \neq \mathbf{u}(t_0^+) \text{ and } \mathbf{v}(t_0) \neq \mathbf{v}(t_0^+) \tag{2}$$

where superscript (+) denotes the right limit of time t_0 as shown in Fig. 1.

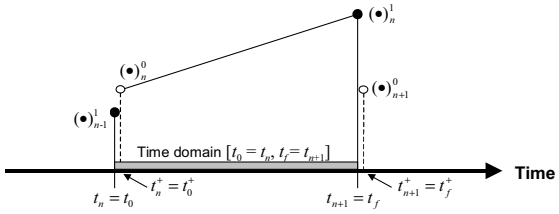

Figure 1 : Description of time domain and jumps of variables.

As a result, the above relations incorporates the jump due to shock loading condition. By the same method, the acceleration-velocity relations are written as follows:

$$\int_{t_0}^{t_f} \mathbf{w}^T \mathbf{a} dt = -\int_{t_0}^{t_f} \dot{\mathbf{w}}^T \mathbf{v} dt + \mathbf{w}^T \mathbf{v}\Big|_{t_0}^{t_f} \text{ for all } \mathbf{w}(t) \tag{3}$$

$$\mathbf{v}(t_0) \neq \mathbf{v}(t_0^+) \text{ and } \mathbf{a}(t_0) \neq \mathbf{a}(t_0^+) \tag{4}$$

The acceleration vector is denoted by **a**. In contrast with dynamic field variables (i.e. **u**, **v**, and **a**), test function **w** is assumed to be continuous at t_0 to ensure the smoothness of the test function.

For the temporal approximation, the time domain of the investigation is restricted to $[t_n = t_0,\ \ t_{n+1} = t_f]$ and the

linear Lagrange interpolation functions are used to approximate displacement $\mathbf{u}$, velocity $\mathbf{v}$, acceleration $\mathbf{a}$, and test function $\mathbf{w}$. The approximation vectors defined on an interval $t_n < t \le t_{n+1} = t + \Delta t$ are written in the following forms.

$$\begin{aligned} \mathbf{u}(t) &= \sum_{i=0}^{1} \psi_i(t)\mathbf{u}_n^i, \quad \mathbf{v}(t) = \sum_{i=0}^{1} \psi_i(t)\mathbf{v}_n^i \\ \mathbf{a}(t) &= \sum_{i=0}^{1} \psi_i(t)\mathbf{a}_n^i, \quad \mathbf{w}(t) = \sum_{i=0}^{1} \psi_i(t)\mathbf{w}_n^i \\ \psi_0(t) &= (t_{n+1} - t)/(t_{n+1} - t_n) \\ \psi_1(t) &= (t - t_n)/(t_{n+1} - t_n) \end{aligned} \tag{5}$$

where $(\bullet)_n^0$ and $(\bullet)_n^1$ denote field values at time t_n^+ and t_{n+1}, respectively. They are shown in Fig. 1. For a higher order approximation, higher order interpolation functions can be used. [Kim, Cho, and Kim (1997), Kim and Cho (1997)]. By substituting interpolating functions (5) into equations (1) and (3), approximated relations for the time derivative are obtained. The relations are written as follows through reordering:

For all $\mathbf{w}_n^i (i = 0, 1)$,

$$\begin{aligned} &\sum_{j=0}^{1} \int_{t_n}^{t_{n+1}} \dot{\psi}_i \psi_j \mathbf{w}_n^{i^T} \mathbf{u}_n^j dt - \mathbf{w}^T \mathbf{u}\Big|_{t_{n+1}} \\ &= -\sum_{j=0}^{1} \int_{t_n}^{t_{n+1}} \psi_i \psi_j \mathbf{w}_n^{i^T} \mathbf{v}_n^j dt - \mathbf{w}^T \mathbf{u}\Big|_{t_n} \\ &\sum_{j=0}^{1} \int_{t_n}^{t_{n+1}} \dot{\psi}_i \psi_j \mathbf{w}_n^{i^T} \mathbf{v}_n^j dt - \mathbf{w}^T \mathbf{v}\Big|_{t_{n+1}} \\ &= -\sum_{j=0}^{1} \int_{t_n}^{t_{n+1}} \psi_i \psi_j \mathbf{w}_n^{i^T} \mathbf{a}_n^j dt - \mathbf{w}^T \mathbf{v}\Big|_{t_n} \end{aligned} \tag{6}$$

where

$$\begin{aligned} &\mathbf{u}(t_n) = \mathbf{u}_{n-1}^1,\ \mathbf{v}(t_n) = \mathbf{v}_{n-1}^1,\ \mathbf{a}(t_n) = \mathbf{a}_{n-1}^1,\ \mathbf{w}(t_n) = \mathbf{w}_n^0 \\ &\mathbf{u}(t_{n+1}) = \mathbf{u}_n^1,\ \mathbf{v}(t_{n+1}) = \mathbf{v}_n^1,\ \mathbf{a}(t_{n+1}) = \mathbf{a}_n^1,\ \mathbf{w}(t_{n+1}) = \mathbf{w}_n^1 \end{aligned}$$

In equation (6), the dynamic field variables $\mathbf{u}$, $\mathbf{v}$, and $\mathbf{a}$ contain the discontinuities at the initial time t_0 (= t_n). $\mathbf{u}_{n-1}^1$, $\mathbf{v}_{n-1}^1$, and $\mathbf{a}_{n-1}^1$ are the given initial vectors obtained from the previous time step. The effect of the initial condition is weakly imposed via $\mathbf{u}_{n-1}^1$,$\mathbf{v}_{n-1}^1$, and $\mathbf{a}_{n-1}^1$. Since equation (6) must hold for all $\mathbf{w}_n^i$, it can be written in simplified matrix form as

$$\begin{aligned} \hat{\Phi}\mathbf{U}_{n+1} &= \Phi\mathbf{V}_{n+1} + \Theta\mathbf{U}_n \\ \hat{\Phi}\mathbf{V}_{n+1} &= \Phi\mathbf{A}_{n+1} + \Theta\mathbf{V}_n \end{aligned} \tag{7}$$

where,

$$\mathbf{U}_{n+1} = \left\{ \mathbf{u}_n^{0^T}, \mathbf{u}_n^{1^T} \right\}^T,\ \mathbf{V}_{n+1} = \left\{ \mathbf{v}_n^{0^T}, \mathbf{v}_n^{1^T} \right\}^T,$$
$$\mathbf{A}_{n+1} = \left\{ \mathbf{a}_n^{0^T}, \mathbf{a}_n^{1^T} \right\}^T$$

The alternative forms for displacement-velocity and velocity-acceleration relations are obtained by multiplying the inverse matrix of $\hat{\Phi}$.

$$\begin{aligned} \mathbf{U}_{n+1} &= \overline{\Psi}\mathbf{V}_{n+1} + \overline{\Psi}_0\mathbf{V}_n + \mathbf{J}\mathbf{U}_n \\ \mathbf{V}_{n+1} &= \overline{\Psi}\mathbf{A}_{n+1} + \overline{\Psi}_0\mathbf{A}_n + \mathbf{J}\mathbf{V}_n \end{aligned} \tag{8}$$

where $\overline{\Psi} = \hat{\Phi}^{-1}\Phi$, $\overline{\Psi}_0 = \mathbf{0}$, $\mathbf{J} = \hat{\Phi}^{-1}\Theta$. Using the discrete operators of equation (8), the numerical time integration algorithm is constructed along with the dynamic equilibrium equation. The equilibrium equation of dynamic systems discretized in space domain is generally given as follows:

$$\mathbf{m}\mathbf{a} + \mathbf{c}\mathbf{v} + \mathbf{k}\mathbf{u} = \mathbf{f} \tag{9}$$

where $\mathbf{m}$, $\mathbf{c}$, and $\mathbf{k}$ are the mass, damping, and stiffness matrices, respectively. The external force vector is denoted by $\mathbf{f}$. With the obtained discrete operator (8), the dynamic equilibrium equations at the inner time steps (i.e. t_n^+ and t_{n+1}) are considered to obtain a time integration algorithm:

$$\mathbf{m}\mathbf{a}_n^i + \mathbf{c}\mathbf{v}_n^i + \mathbf{k}\mathbf{u}_n^i = \mathbf{f}_n^i,\ (i = 0, 1) \tag{10}$$

Using the matrix notation, it can be denoted as

$$\mathbf{M}\mathbf{A}_{n+1} + \mathbf{C}\mathbf{V}_{n+1} + \mathbf{K}\mathbf{U}_{n+1} = \mathbf{F}_{n+1} \tag{11}$$

where $\mathbf{M}$, $\mathbf{C}$, and $\mathbf{K}$ are block diagonal matrices for mass, damping, and stiffness, respectively, and $\mathbf{F}$ denotes the forcing vector. To obtain the dynamic field variables $\mathbf{A}_{n+1}$, $\mathbf{V}_{n+1}$, and $\mathbf{U}_{n+1}$, it is sufficient to solve the equations (8) and (11), simultaneously.

By substituting equation (8) into equation (11), equation (11) can be rewritten in terms of acceleration as follows:

$$(\mathbf{M} + \mathbf{C}\overline{\Psi} + \mathbf{K}\overline{\Psi}^2)\mathbf{A}_{n+1} = \mathbf{F} - \mathbf{C}\tilde{\mathbf{V}}_{n+1}^{(\mathbf{a})} - \mathbf{K}\tilde{\mathbf{U}}_{n+1}^{(\mathbf{a})} \tag{12}$$

where,

$$\begin{aligned} \tilde{\mathbf{U}}_{n+1}^{(\mathbf{a})} &= \overline{\Psi}\overline{\Psi}_0\mathbf{A}_n + (\overline{\Psi}\mathbf{J} + \overline{\Psi}_0)\mathbf{V}_n + \mathbf{J}\mathbf{U}_n \\ \tilde{\mathbf{V}}_{n+1}^{(\mathbf{a})} &= \overline{\Psi}_0\mathbf{A}_n + \mathbf{J}\mathbf{V}_n \end{aligned}$$

where $\tilde{\mathbf{U}}_{n+1}^{(\mathbf{a})}$ and $\tilde{\mathbf{V}}_{n+1}^{(\mathbf{a})}$ are predictors for displacement and velocity, respectively. The predictor-corrector algorithm that is based on the acceleration form can be written as follows. The detail derivation procedure for the algorithm is similar to that in the paper of [Kim, Cho and Kim (1997)].

i) Calculate $\mathbf{a}_0$ such that $\mathbf{ma}_0+\mathbf{cv}_0+\mathbf{ku}_0=\mathbf{f}_0$
Set $\mathbf{A}_0=\{\mathbf{0}^T,\mathbf{a}_0^T\}^T,\mathbf{V}_0=\{\mathbf{0}^T,\mathbf{v}_0^T\}^T,\mathbf{U}_0=\{\mathbf{0}^T,\mathbf{u}_0^T\}^T$

ii) Calculate $\mathbf{M}^{eff}=\mathbf{M}+\mathbf{C}\overline{\Psi}+\mathbf{K}\overline{\Psi}^2$ and $\mathbf{M}^{eff^{-1}}$

iii) Do n = 0

$$\text{Predict}\quad\begin{cases}\tilde{\mathbf{U}}_{n+1}^{(\mathbf{a})}=\overline{\Psi\Psi}_0\mathbf{A}_n+(\overline{\Psi}\mathbf{J}+\overline{\Psi}_0)\mathbf{V}_n+\mathbf{J}\mathbf{U}_n\\ \tilde{\mathbf{V}}_{n+1}^{(\mathbf{a})}=\overline{\Psi}_0\mathbf{A}_n+\mathbf{J}\mathbf{V}_n\end{cases}\tag{13}$$

$$\text{Calculate}\quad\begin{cases}\mathbf{R}_{n+1}^{(\mathbf{a})}=\mathbf{F}_{n+1}-\mathbf{C}\tilde{\mathbf{V}}_{n+1}^{(\mathbf{a})}-\mathbf{K}\tilde{\mathbf{U}}_{n+1}^{(\mathbf{a})}\\ \mathbf{A}_{n+1}=\mathbf{M}^{eff^{-1}}\mathbf{R}_{n+1}^{(\mathbf{a})}\end{cases}\tag{14}$$

$$\text{Correct}\quad\begin{cases}\mathbf{U}_{n+1}=\tilde{\mathbf{U}}_{n+1}^{(\mathbf{a})}+\overline{\Psi}^2\mathbf{A}_{n+1}\\ \mathbf{V}_{n+1}=\tilde{\mathbf{V}}_{n+1}^{(\mathbf{a})}+\overline{\Psi}\mathbf{A}_{n+1}\end{cases}\tag{15}$$

Set n = n+1

Continue

After the initialization and predictor stages, the accelerations are obtained through equation (14). The displacement and velocity are corrected by the correction equation (15).

3 Explicit Solution Procedure

In the discontinuous time integration method, equilibrium conditions are considered at the next time step to obtain a solution at the next time step as described in equation (11). The stiffness matrix **K** and the damping matrix **C** induce the coupling between the solutions at time t_{n+1} even if a mass lumping technique is chosen in the equation (12). The coupling can be eliminated only when the second and the third terms on the left-hand side of the equation (12) are evaluated by the given dynamic field variables. Although it is impossible to evaluate the terms exactly by only the given values at previous time t_n, we can approximate the terms by using the information obtained at the previous time step. Towards the end, the following procedure is devised to eliminate the coupling between the unknown variables at time t_{n+1}. At first, the following intermediate equilibrium equation is considered to find an approximated value $\mathbf{A}_{n+1}^*$ for acceleration $\mathbf{A}_{n+1}$.

$$\mathbf{MA}_{n+1}^*=\mathbf{F}_{n+1}-(\mathbf{C}\tilde{\mathbf{V}}_{n+1}^{(\mathbf{a})}+\mathbf{K}\tilde{\mathbf{U}}_{n+1}^{(\mathbf{a})})\tag{16}$$

Because **M** is a diagonal matrix, $\mathbf{A}_{n+1}^*$ in equation (16) can be readily obtained. Secondly, the term $(\mathbf{C}\overline{\Psi}+\mathbf{K}\overline{\Psi}^2)\mathbf{A}_{n+1}$ in implicit equation (12) is replaced by $(\mathbf{C}\overline{\Psi}+\mathbf{K}\overline{\Psi}^2)\mathbf{A}_{n+1}^*$, and the following equation (17) is solved for $\mathbf{A}_{n+1}$.

$$\mathbf{MA}_{n+1}=\mathbf{F}_{n+1}-(\mathbf{C}\tilde{\mathbf{V}}_{n+1}^{(\mathbf{a})}+\mathbf{K}\tilde{\mathbf{U}}_{n+1}^{(\mathbf{a})})-(\mathbf{C}\overline{\Psi}+\mathbf{K}\overline{\Psi}^2)\mathbf{A}_{n+1}^*\tag{17}$$

And finally, the predicted displacement and velocity are corrected by using equation (15).

It is noted again that the algorithm does not need any matrix factorization process when a lumped mass matrix is adopted. The explicit solution procedure of the discontinuous time integration method can be summarized as follows:

i) Calculate $\mathbf{a}_0$ such that $\mathbf{ma}_0+\mathbf{cv}_0+\mathbf{ku}_0=\mathbf{f}_0$;
$\{\mathbf{a}_0\}_i=\{\mathbf{f}_0-\mathbf{cv}_0-\mathbf{ku}_0\}_i/[\mathbf{m}]_{ii}$
Set $\mathbf{A}_0=\{\mathbf{0}^T,\mathbf{a}_0^T\}^T,\mathbf{V}_0=\{\mathbf{0}^T,\mathbf{v}_0^T\}^T,\mathbf{U}_0=\{\mathbf{0}^T,\mathbf{u}_0^T\}^T$

ii) Do n = 0

$$\text{Predict}\quad\begin{cases}\tilde{\mathbf{U}}_{n+1}^{(\mathbf{a})}=\overline{\Psi\Psi}_0\mathbf{A}_n+(\overline{\Psi}\mathbf{J}+\overline{\Psi}_0)\mathbf{V}_n+\mathbf{J}\mathbf{U}_n\\ \tilde{\mathbf{V}}_{n+1}^{(\mathbf{a})}=\overline{\Psi}_0\mathbf{A}_n+\mathbf{J}\mathbf{V}_n\end{cases}\tag{18}$$

$$\text{Calculate}\quad\begin{cases}\mathbf{R}_{n+1}^{(\text{explicit})}=\mathbf{F}_{n+1}-(\mathbf{C}\tilde{\mathbf{V}}_{n+1}^{(\mathbf{a})}+\mathbf{K}\tilde{\mathbf{U}}_{n+1}^{(\mathbf{a})})\\ \{\mathbf{A}_{n+1}^*\}_i=\dfrac{\{\mathbf{R}_{n+1}^{(\text{explicit})}\}_i}{[\mathbf{M}]_{ii}}\end{cases}\tag{19}$$

$$\text{Correct}\quad\begin{cases}\{\mathbf{A}_{n+1}\}_i=\dfrac{\{\mathbf{R}_{n+1}^{(\text{explicit})}-(\mathbf{C}\overline{\Psi}+\mathbf{K}\overline{\Psi}^2)\mathbf{A}_{n+1}^*\}_i}{[\mathbf{M}]_{ii}}\end{cases}\tag{20}$$

$$\text{Correct}\quad\begin{cases}\mathbf{U}_{n+1}=\tilde{\mathbf{U}}_{n+1}^{(\mathbf{a})}+\overline{\Psi}^2\mathbf{A}_{n+1}\\ \mathbf{V}_{n+1}=\tilde{\mathbf{V}}_{n+1}^{(\mathbf{a})}+\overline{\Psi}\mathbf{A}_{n+1}\end{cases}\tag{21}$$

Set $n = n+1$

Continue

where $\{\bullet\}_i$ means components of vector and $[\bullet]_{ii}$ denotes the diagonal elements of matrix.

The proposed algorithm is a two-stage correction scheme. Through the first correction stage, the acceleration is updated and the corrected acceleration is used in the correction of displacement and velocity.

4 Stability

The stability analysis is carried out to identify whether the proposed explicit solution procedure is stable or not. In the stability analysis, all of the acceleration, velocity, and displacements are used as a system state vector χ.

The equilibrium condition, which is used in the proposed explicit algorithm, is represented by equations (16) and (17). Substituting equation (16) into equation (17) yields the following equilibrium condition.

$$\begin{aligned}&\mathbf{M}\mathbf{A}_{n+1}+(\mathbf{C}\overline{\Psi}+\mathbf{K}\overline{\Psi}^2)\mathbf{M}^{-1}(\mathbf{F}_{n+1}-(\mathbf{C}\tilde{\mathbf{V}}^{(\mathbf{a})}_{n+1}+\mathbf{K}\tilde{\mathbf{U}}^{(\mathbf{a})}_{n+1}))\\&=\mathbf{F}_{n+1}-(\mathbf{C}\tilde{\mathbf{V}}^{(\mathbf{a})}_{n+1}+\mathbf{K}\tilde{\mathbf{U}}^{(\mathbf{a})}_{n+1}))\end{aligned} \tag{22}$$

Consider a system with no damping and no external loading for the stability analysis. Then equation (22) is reduced to

$$\mathbf{M}\mathbf{A}_{n+1}=-(\mathbf{K}-\mathbf{K}\overline{\Psi}^2\mathbf{M}^{-1}\mathbf{K})\tilde{\mathbf{U}}^{(\mathbf{a})}_{n+1} \tag{23}$$

If the predictor for displacement $\tilde{\mathbf{U}}^{(\mathbf{a})}_{n+1}$ in equation (23) is expressed in terms of the variables $\mathbf{U}_n$, $\mathbf{V}_n$, and $\mathbf{A}_n$ at time t_n by using equation (18), equation (23) results in the form of

$$\mathbf{M}\mathbf{A}_{n+1}=-\mathbf{Y}\overline{\Psi\Psi}_0\mathbf{A}_n-\mathbf{Y}(\overline{\Psi}\mathbf{J}+\overline{\Psi}_0)\mathbf{V}_n-\mathbf{Y}\mathbf{J}\mathbf{U}_n \tag{24}$$

where $\mathbf{Y}=(\mathbf{K}-\mathbf{K}\overline{\Psi}^2\mathbf{M}^{-1}\mathbf{K})$. In order to construct a system evolution equation, the equilibrium condition (24) is used together with the velocity-displacement and the acceleration-velocity relations shown in equation (8). (It is noted that equation (8) is an alternative form of correction equation (21).) The system evolution equation can be written as the following matrix form.

$$\begin{aligned}&\begin{bmatrix}\mathbf{M}&\mathbf{0}&\mathbf{0}\\-\overline{\Psi}&\mathbf{I}&\mathbf{0}\\\mathbf{0}&-\overline{\Psi}&\mathbf{I}\end{bmatrix}\begin{Bmatrix}\mathbf{A}_{n+1}\\\mathbf{V}_{n+1}\\\mathbf{U}_{n+1}\end{Bmatrix}\\&=\begin{bmatrix}-\mathbf{Y}\overline{\Psi}\overline{\Psi}_0&-\mathbf{Y}(\overline{\Psi}\mathbf{J}+\overline{\Psi}_0)&-\mathbf{Y}\mathbf{J}\\\overline{\Psi}_0&\mathbf{J}&\mathbf{0}\\\mathbf{0}&\overline{\Psi}_0&\mathbf{J}\end{bmatrix}\begin{Bmatrix}\mathbf{A}_n\\\mathbf{V}_n\\\mathbf{U}_n\end{Bmatrix}\end{aligned} \tag{25}$$

It is denoted in simplified form as

$$\hat{\mathbf{T}}\chi(t_{n+1})=\hat{\mathbf{T}}_0\chi(t_n) \tag{26}$$

where the system state vector χ consists of the acceleration, velocity, and displacement. To observe the stability characteristics of the proposed method, a single degree of freedom system is adopted and the corresponding generalized eigenvalue problem is solved to find the amplification factor [Cho and Kim (1999)]. Stability is guaranteed when the amplification factor (magnitude of eigenvalue of the system evolution equation) is less than or equal to 1.

The calculated amplification factors for the proposed explicit solution procedure are shown in Fig. 2. From the results of Fig. 2, it is observed that the amplification factors are less than or equal to unity in the region of $\Delta t \leq 0.353T$. The scissors in Fig. 2 denotes the boundary between the stable and unstable regions. Therefore, stability is ensured for that region of Δt. It means that the conditional stability is guaranteed for the present explicit method.

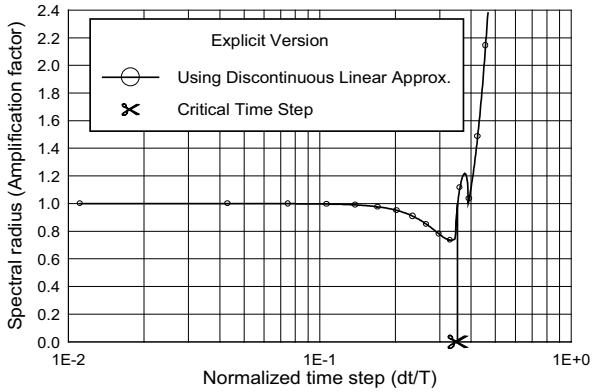

Figure 2 : Amplification factor of the present explicit method (using linear approximation in time domain)

The critical time step for the present explicit method is about 0.353 times that of the period (i.e. $\Delta t_{cr} \approx 0.353T$). To ensure the stability for a system having multi-degrees of freedom, the stability condition should be satisfied for all dynamic modes of the system. Therefore, the critical time step should satisfy the following condition.

The present explicit method (Linear Approximation in Time)

$$\Delta t_{cr} \leq 0.353 T_{\min} = 0.353 \times \frac{2\pi}{\omega_{\max}} \tag{27}$$

The central difference method

$$\Delta t_{cr} \leq 0.318 T_{\min} = 0.318 \times \frac{2\pi}{\omega_{\max}} \tag{28}$$

where T_{min} and ω_{max} mean the minimum period and the maximum frequency of the considered dynamic system, respectively.

The result shows that the critical time step of the proposed method is relatively large compared with critical time step $T/\pi \approx 0.318T$ of the central difference method [Bathe (1996)]. Therefore, a time step larger than the central difference method can be adopted in the present method without loss of stability.

To observe the accuracy of the present explicit algorithm, a free-oscillation problem having unit mass and unit stiffness is solved using the present explicit solution procedure. Two cases of initial conditions are imposed. One is $u(0) = 1, v(0) = 0$, the other is $u(0) = 0, v(0) = 1$. The displacement convergence rate of the present explicit algorithm is shown in Fig. 3 for each case. The slope of the curve denotes the order of convergence. The displacement error e_{disp} is calculated by the difference of numerically calculated displacement $u_{num}(2\pi)$ and exact solution $u(2\pi)$ at $t = 2\pi$ as

$$e_{disp} = \|u_{num}(2\pi) - u(2\pi)\| \tag{29}$$

The results in Fig. 3 show that the present explicit time integration algorithm (linear approximation in time domain) has a third order convergence in the first case (imposition of the initial displacement) and a fourth order convergence in the second case (imposition of the initial velocity). Therefore the present method has the third order convergence at least in combined cases.

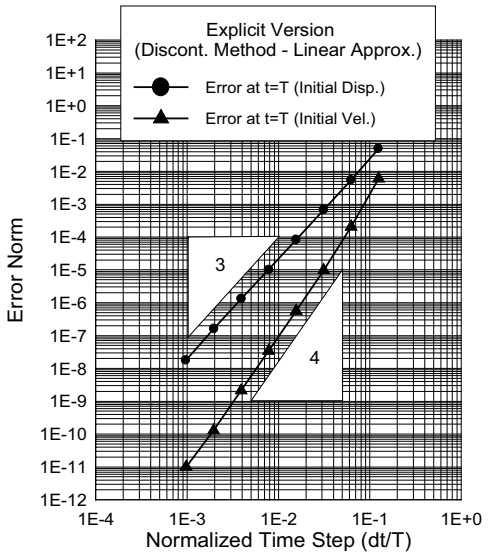

Figure 3 : Log-scale plot of error norm vs. normalized time step (The present explicit time intergration method – using linear approximation in time domain)

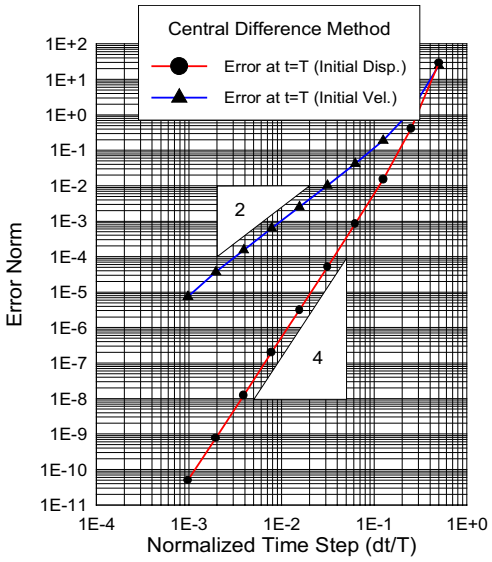

Figure 4 : Log-scale plot of error norm vs. normalized time step (The central difference method)

From the results, it is confirmed that the proposed explicit time integration algorithm with linear approximation in time domain preserves the third order convergence of the discontinuous time integration method [Cho and

Kim (1999)], and it is more accurate than the central difference method which has a second order convergence as shown in Fig. 4.

5 Dynamic-Contact/Impact Problems

In this section, the way to implement the proposed explicit procedure in analyzing dynamic-contact/impact problems is briefly described, and numerical tests are carried out to identify the validity of the proposed explicit solution procedure.

Algorithm

Through the finite element approximation along with the exterior penalty method, dynamic-contact/ impact problems result in the following dynamic equilibrium equation (30) at the inner time steps. Detailed derivation can be found in a Cho and Kim (1999).

$$\mathbf{m}\mathbf{a}_n^i+(\mathbf{k}+\frac{1}{\varepsilon_p}\mathbf{k}_\mathbf{N}(\mathbf{u}_n^i))\mathbf{u}_n^i=\mathbf{f}_n^i-\frac{1}{\varepsilon_p}\mathbf{f}_\mathbf{N}(\mathbf{u}_n^i),\ (i=0,1) \quad (30)$$

where ε_p denotes the penalty parameter, and subscript N means that the term comes from the contact effect. Using the matrix notation, it can be rewritten as follows.

$$\mathbf{M}\mathbf{A}_{n+1}=\mathbf{F}_{n+1}+\mathbf{F}_\mathbf{N}(\mathbf{U}_{n+1})-(\mathbf{K}+\mathbf{K}_\mathbf{N}(\mathbf{U}_{n+1}))\mathbf{U}_{n+1} \quad (31)$$

As described before, the intermediate acceleration $\mathbf{A}_{n+1}^*$ can be obtained from the following equation.

$$\mathbf{M}\mathbf{A}_{n+1}^*=\mathbf{F}_{n+1}+\mathbf{F}_\mathbf{N}(\tilde{\mathbf{U}}_{n+1}^{(\mathbf{a})})-(\mathbf{K}+\mathbf{K}_\mathbf{N}(\tilde{\mathbf{U}}_{n+1}^{(\mathbf{a})}))\tilde{\mathbf{U}}_{n+1}^{(\mathbf{a})} \quad (32)$$

After the intermediate acceleration $\mathbf{A}_{n+1}^*$ is obtained by solving equation (32), it is used for the correction of acceleration. The correction equation (35) for acceleration is constructed by the same procedure described in the previous section. The algorithm is summarized below.

i) *Calculate* $\mathbf{a}_0$ *such that*
$\mathbf{m}\mathbf{a}_0+(\mathbf{k}+\frac{1}{\varepsilon_p}\mathbf{k}_\mathbf{N}(\mathbf{u}_0))\mathbf{u}_0=\mathbf{f}_0-\frac{1}{\varepsilon_p}\mathbf{f}_\mathbf{N}(\mathbf{u}_0)$
Set $\mathbf{A}_0=\{\mathbf{0}^T,\mathbf{a}_0^T\}^T, \mathbf{V}_0=\{\mathbf{0}^T,\mathbf{v}_0^T\}^T$,
$\mathbf{U}_0=\{\mathbf{0}^T,\mathbf{u}_0^T\}^T$

ii) Do n=0
Predict

$$\begin{cases}\tilde{\mathbf{U}}_{n+1}^{(\mathbf{a})}=\overline{\Psi}\overline{\Psi}_0\mathbf{A}_n+(\overline{\Psi}\mathbf{J}+\overline{\Psi}_0)\mathbf{V}_n+\mathbf{J}\mathbf{U}_n\\ \tilde{\mathbf{V}}_{n+1}^{(\mathbf{a})}=\overline{\Psi}_0\mathbf{A}_n+\mathbf{J}\mathbf{V}_n\end{cases} \quad (33)$$

Calculate

$$\begin{cases}\mathbf{R}_{n+1}^{(\text{explicit})}=\mathbf{F}_{n+1}+\mathbf{F}_\mathbf{N}(\tilde{\mathbf{U}}_{n+1}^{(\mathbf{a})})-(\mathbf{K}+\mathbf{K}_\mathbf{N}(\tilde{\mathbf{U}}_{n+1}^{(\mathbf{a})}))\tilde{\mathbf{U}}_{n+1}^{(\mathbf{a})}\\ \{\mathbf{A}_{n+1}^*\}_i=\dfrac{\{\mathbf{R}_{n+1}^{(\text{explicit})}\}_i}{[\mathbf{M}]_{ii}}\end{cases} \quad (34)$$

Correct

$$\begin{cases}\{\mathbf{A}_{n+1}\}_i=\dfrac{\{\mathbf{R}_{n+1}^{(\text{explicit})}-(\mathbf{K}+\mathbf{K}_\mathbf{N}(\tilde{\mathbf{U}}_{n+1}^{(\mathbf{a})}))\overline{\Psi}^2\mathbf{A}_{n+1}^*\}_i}{[\mathbf{M}]_{ii}}\end{cases} \quad (35)$$

Correct

$$\begin{cases}\mathbf{U}_{n+1}=\tilde{\mathbf{U}}_{n+1}^{(\mathbf{a})}+\overline{\Psi}^2\mathbf{A}_{n+1}\\ \mathbf{V}_{n+1}=\tilde{\mathbf{V}}_{n+1}^{(\mathbf{a})}+\overline{\Psi}\mathbf{A}_{n+1}\end{cases} \quad (36)$$

Set $n = n+1$
Continue

If a lumped mass matrix is chosen, the above procedure produces the next time solution directly without any factorization and iteration. It is noted that the nonlinear stiffness matrix $\mathbf{K}_\mathbf{N}$ in (35) may also be evaluated at $\mathbf{U}_{n+1}^*(\equiv\tilde{\mathbf{U}}_{n+1}^{(\mathbf{a})}+\overline{\Psi}^2\mathbf{A}_{n+1}^*)$, but it needs additional computational efforts. Therefore, the nonlinear stiffness matrix $\mathbf{K}_\mathbf{N}$ evaluated at $\tilde{\mathbf{U}}_{n+1}^{(\mathbf{a})}$ is used in the current examples.

Bar Impact Problem

By using the proposed explicit algorithm, the bar impact problem in Fig. 5 was analyzed. The predicted results were compared with the results obtained by the central difference method because the central difference method is widely used in explicit dynamic analysis. The material properties and the dimensions of model are shown in table 1.

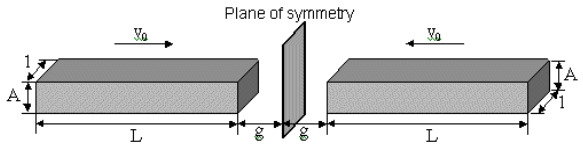

Figure 5 : Impact of two identical bars

The contact force obtained by the analytical method is 2×10^6N in 0 μsec $\le t \le$ 60 μsec and zero in $t >$ 60μsec.

Table 1 : Material properties and dimensions of bar

E = 100 GPa	A = 2 cm	g = 0 cm
ρ = 1000 kg/m^3	L = 30 cm	v_0= 10 m/sec

For a finite element discretization of bar, two hundred linear bar elements were used. The row-sum technique [Hughes (1987)] was used to construct a lumped mass matrix.

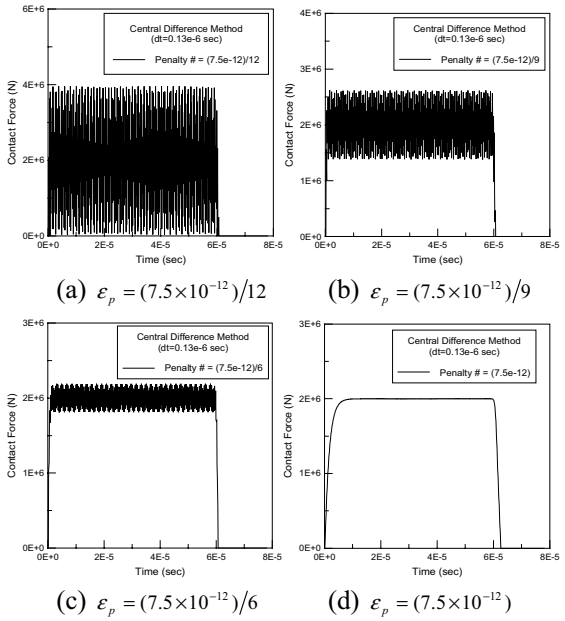

(a) $\varepsilon_p = (7.5\times10^{-12})/12$ (b) $\varepsilon_p = (7.5\times10^{-12})/9$

(c) $\varepsilon_p = (7.5\times10^{-12})/6$ (d) $\varepsilon_p = (7.5\times10^{-12})$

Figure 6 : Contact force histories according to penalty parameters (by the central difference method)

The results shown in Fig. 6 and Fig. 7 were computed with several penalty parameters by the central difference method and the proposed algorithm, respectively. In all the simulations presented in Fig. 6 and 7, time step size of 0.13 μsec was used. The selected penalty parameters are 7.5×10^{-12}, $(7.5\times10^{-12})/6$, $(7.5\times10^{-12})/9$, and $(7.5\times10^{-13})/12$. As the penalty parameter is decreased, the central difference method produces an undesirable oscillation; however, the proposed explicit algorithm gives a relatively stable solution for small penalty parameters compared to the central difference method. Moreover, by comparing the contact force histories, which have no undesirable oscillation, it is observed that the proposed method gives more accurate contact durations than the central difference method.

In Fig. 8, the displacement of contact node is plotted. For

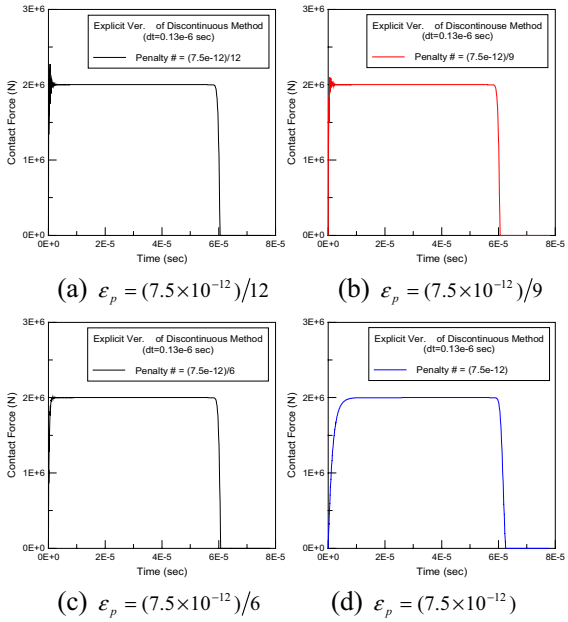

(a) $\varepsilon_p = (7.5\times10^{-12})/12$ (b) $\varepsilon_p = (7.5\times10^{-12})/9$

(c) $\varepsilon_p = (7.5\times10^{-12})/6$ (d) $\varepsilon_p = (7.5\times10^{-12})$

Figure 7 : Contact force histories according to penalty parameters (by the present explicit method)

the central difference method, the result of penalty parameter 7.5×10^{-12} is presented, since the contact force of that is not oscillatory. For the proposed explicit algorithm, the result of penalty parameter $(7.5\times10^{-12})/6$ is presented due to the same reason. From the results, it is observed that the result of the proposed algorithm has less penetration than that of the central difference method.

The contact force history in Fig. 9 is predicted with time step 0.15 μsec and penalty parameter $(7.5\times10^{-12})/3$ through the proposed method. The contact force history, predicted by the central difference method with the same time step and the same penalty parameter, is shown in Fig. 10. The figure shows that the solution from the central difference method is increased without bound, while the solution obtained by the proposed explicit method is stable and accurate as shown in Fig. 9. The results show that a larger time step size can be adopted in the proposed explicit algorithm than in the central difference method without loss of stability.

From the simulation results, it was confirmed that the proposed explicit algorithm gives more reliable solutions than the central difference method. Moreover, a larger time step size can be used in the proposed algorithm than in the central difference method.

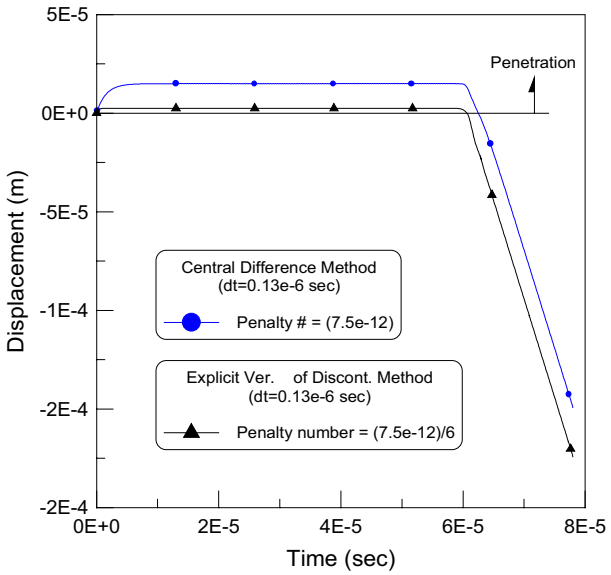

Figure 8 : Displacement history of contact node

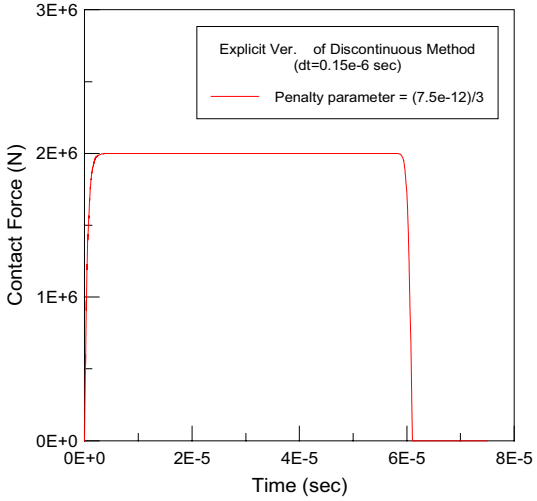

Figure 9 : Contact force history by the proposed algorithm with the time step $\Delta t = 0.15\mu$sec

Impact between Isotropic Solid and Rigid Cylinder

To confirm the validity of the proposed explicit method, two-dimensional impact behaviors between isotropic solid and rigid cylinders were visited. Since the analytical solution is not available, the computed results were compared with those obtained by the implicit discontinuous time integration method. The material properties and the dimensions for the model problem are presented in Table 2.

In Table 2, L is length, A is thickness, m is the mass of impactor, v_0 is the initial velocity of impactor, and R is the radius of impactor. Due to the symmetric nature of model problem, half of the model is discretized as shown in Fig. 11. A four-node plane strain element was adopted for discretization, and the row-sum technique was used to obtain a lumped mass matrix. The total number of elements used in the finite element model was 1600, and the total number of nodes was 1681. For time integration, 0.035 μsec of time step was chosen. As boundary conditions, it was assumed that the bottom is fixed in the y-direction and both sides are fixed in the x-direction.

Table 2 : Material properties and dimensions of a solid block and rigid cylinder

E=70Gpa	$\nu = 0.3$	ρ = 2710 kg/m^3	L = 2 cm
A=1 cm	R = 1 cm	m = 65.8 g	v_0= 10 m/s

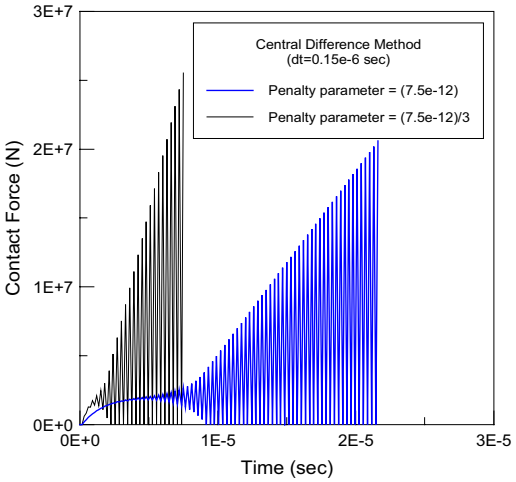

Figure 10 : Contact force history by the central difference method with the time step $\Delta t = 0.15\mu$sec

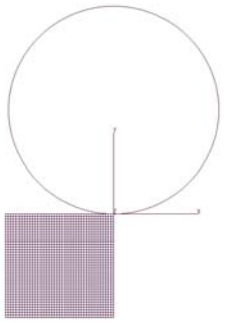

Figure 11 : Finite Element Model

To impose the contact condition, a penalty parameter of 0.15×10^{-14} was selected, based on the penalty parameter study. Solution convergence according to penalty parameter is shown in Fig. 12.

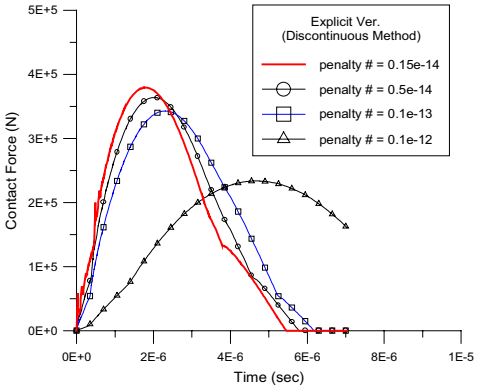

Figure 12 : Solution convergence according to penalty parameter

Fig. 13 shows contact force histories obtained by the present explicit solution procedure and the implicit discontinuous time integration method [Cho and Kim (1999)]. Comparing the results, it was found that the present explicit solution procedure which is a modification of the discontinuous method, gives a reasonable solution while saving of computational costs.

In Fig. 14, the displacement histories of the contact node and impactor are presented. The results show that a slight penetration occurs in the explicit method. It is a shortcoming of explicit method that should be paid for lower computing cost than the implicit method. Fig. 15 shows the velocity histories of the contact node and impactor. If the explicit method is used, there is a little undesirable

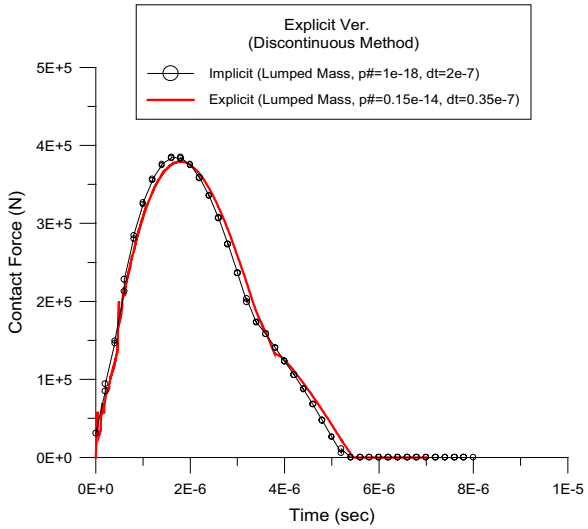

Figure 13 : Comparison of contact force histories from implicit method and explicit method

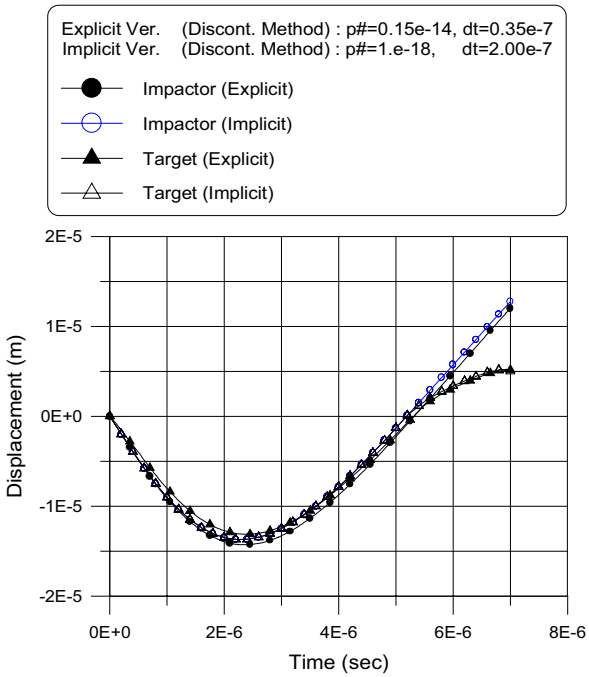

Figure 14 : Displacement histories of contact node and impactor

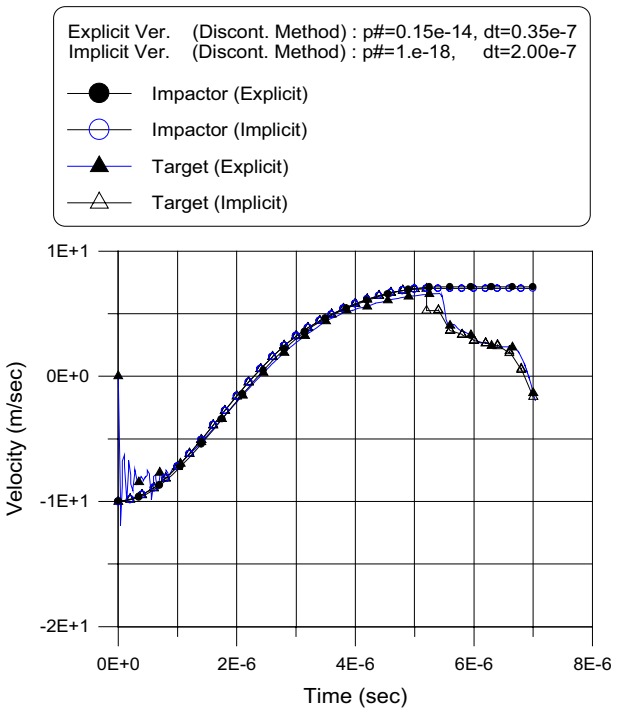

Figure 15 : Velocity histories of contact node and impactor

oscillation at the initial impact stage. However, the spurious oscillation decays rapidly and a stable solution is obtained.

From the numerical tests, it is confirmed that the proposed explicit solution procedure of the discontinuous time integration method is enough to simulate dynamic-contact/impact problems.

6 Conclusions

By modifying the recently developed discontinuous time integration method, a new explicit solution procedure is proposed. In the present explicit discontinuous time integration method, a two-stage correction algorithm was used to avoid any matrix factorization. In this correction routine, an intermediate acceleration is obtained by using an intermediate equilibrium equation, and it is also utilized for obtaining further modified equilibrium condition. After the correction routine, dynamic field variables at the next time step are obtained without any matrix factorization. To observe the stability and accuracy of the proposed explicit solution procedure, stability and accuracy analyses were carried out. The analysis results show that the proposed method gives a larger critical time step and higher order accuracy than the central difference method. During the several numerical tests for dynamic-contact/impact problems, it was observed that the proposed explicit time integration method gives more stable and accurate solutions than the central difference method, which is widely adopted in explicit computations of impact analysis.

Consequently, it is confirmed that the proposed explicit discontinuous time integration method can be efficiently utilized without matrix factorization and iteration in analyzing transient dynamic problems which have shock-type loading conditions such as dynamic-contact/impact problems.

Acknowledgement: The authors would like to acknowledge the financial support from the Ministry of Science and Technology through the National Research Laboratory Programs under the contract number 00-N-NL-01-C-026.

References

Abrate, S. (1991): Impact on Laminated Composite Materials. *Applied Mechanics Reviews*, Vol. 44, No.4, pp. 155-190.

Bathe, K. J. (1996): *Finite Element Procedures.* International Ed., Prentice-Hall, Englewood Cliffs, NJ, Chapter 9.

Borri, M.; Mello, F.; Atluri, S. N. (1990): Variational approaches for dynamics and time-finite-elements: numerical studies, *Computational Mechanics*, Vol. 7, pp 49-76.

Borri, M.; Bottasso, C. (1993): A general framework for interpreting time finite element formulations. *Computational Mechanics*, Vol. 13, pp. 133-142.

Chien, C-C.; Wu, T-Y. (2001): An Advanced Time Discontinuous Galerkin Finite Element Method for Structural Dynamics. *CMES: Computer Modeling in Engineering & Sciences*, Vol. 2, No. 2, pp. 213-226.

Cho, J. Y.; Kim, S. J. (1999): A New Discontinuous Time Integration Method for Dynamic-Contact/Impact Problems. *AIAA Journal*, Vol. 37, No. 7, pp. 874-880.

Goo, N. S.; Kim, S. J. (1997): Dynamic Contact Analysis of Laminated Composite Plates Under Low-Velocity Impact. *AIAA Journal*, Vol. 35, No. 9, pp.1518-1521.

Hughes, T.J.R.; Taylor, R.L.; Sackman, J. L.; Curnier, A.; Kanoknukulchai, W. (1976): A Finite Element Method for a Class of Contact-Impact Problems. *Computer Method in Applied Mechanics and Engineering*, Vol. 8, No. 3, pp.249-276.

Hughes, T. J. R. (1987): *The Finite Element Method - Linear Static and Dynamic Finite Element Analysis*. Prentice Hall, Englewood Cliffs, NJ, , Chap. 9.

Hulbert, G. M.; Hughes, T. J. R. (1990): Space-Time Finite Element Methods for Second-Order Hyperbolic Equations. *Computer Methods in Applied Mechanics and Engineering*, Vol. 84, No. 3, pp.327-348.

Kim, S. J.; Cho, J. Y.; Kim, W. D. (1997): From the Trapezoidal rule to Higher Order Accurate and Unconditionally Stable Time Integration Method for Structural Dynamics. *Computer Method in Applied Mechanics and Engineering*, Vol.149, pp. 73-88.

Kim, S. J.; Cho, J. Y. (1997): Penalized Weighted Residual Method for the Initial Value Problems. *AIAA Journal*, Vol. 35, No.1, pp.172-177.

Lee, K. (1994): A Numerical solution for Dynamic Contact Problems satisfying the Velocity and Acceleration Compatibilities on the Contact Surface. *Computational Mechanics*, Vol. 15, No. 3, pp. 189-200.

Reddy, B. D. (1986): *Functional Analysis and Boundary-Value Problems: an Introductory Treatment*. John Wiley and Sons, New York, Chap. 7.

Taylor, R. L.; Papadopoulos, P. (1993): On a Finite Element Method for Dynamic Contact/Impact Problems. *International Journal for Numerical Methods in Engineering*, Vol. 36, No. 12, pp. 2123-2140.

Zhong, Z. H. (1993): *Finite element Procedures for Contact-Impact Problems*. Oxford University Press, New York, Chap. 4.